Geosciences Journal
Vol. 17, No. 4, p. 403 − 416, December 2013
DOI 10.1007/s12303-013-0035-x

Petrogenetic implications of the mineral-chemical characteristics of scheelite and associated phases from Miniki Gol (Chitral), NW Pakistan

Mohammad Zahid
Mohammad Arif*
Charlie J. Moon

Department of Geology, University of Peshawar, Peshawar 25120, Pakistan
Camborne School of Mines, The University of Exeter, Cornwall Campus, Penryn, Cornwall TR109EZ, UK

ABSTRACT: The stratabound tungsten mineralization in Chitral, northern Pakistan, lies within the Hindu Kush terrane and is located to the north-west of the Main Karakoram Thrust (MKT) that represents the suture zone between the Kohistan complex and Asian plate. The area has undergone amphibolite facies metamorphism followed by retrogression and at least two episodes of deformation. Scheelite occurs mainly in the calc-silicate quartzite and subordinate tourmalinite associated with metapelite of the Jurassic Arkari Formation at Miniki Gol. The scheelite host rocks are intruded by leucogranite, which is exposed ~400 m east of the studied tungsten mineralization. The leucogranite was emplaced after the culmination of the amphibolite facies metamorphism. The scheelite-bearing calc-silicate rock consists of clinozoisite, quartz, calcic-amphibole, plagioclase, chlorite, biotite, calcite, sphene and garnet. This mineral assemblage correlates with a skarn-type environment. Scheelite is intergrown with clinozoisite in the calc-silicate rock and also associated with tourmaline and spessartine-rich garnet in the tourmalinite. The extensive tourmalinisation leading to the formation of abundant (i.e., up to 80 modal%) tourmaline in the scheelite-bearing tourmalinite appears to have been caused by a post-magmatic hydrothermal activity. The mentioned leucogranite in the area might have acted as a source of fluids for this boron-dominated metasomatic process. The abundant development of epidote, making up to 60% by volume of the calc-silicate rock, signifies its formation through a hydrothermal phenomenon. The chemical compositions of tourmaline, clinozoisite, sphene, garnet and scheelite from the calc-silicate rock also support their hydrothermal origin. Similarly, the compositional characteristics of both tourmaline and spessartine-rich garnet from the tourmalinite indicate the precipitation of these phases from evolved acidic magma-derived fluids. More importantly, the investigated scheelite contains significant amounts of Zr (up to 0.46 wt% ZrO_2) and Ta (up to 0.35 wt% Ta_2O_5), which are believed to replace W in scheelite from post-magmatic environments. As all the mentioned minerals are associated and some of them even intergrown with scheelite, it appears that the tungsten mineralization also is genetically linked to the solidification and emplacement of leucogranite in the area. Although itself generally unmineralized, the Miniki Gol leucogranite's average W content (5.3 ppm) is higher than that of low-Ca granites.

Key words: scheelite, mineralization, mineral chemistry, host rocks, petrogenesis

*Corresponding author: arif_pkpk@yahoo.com

1. INTRODUCTION

Stratabound tungsten mineralization in Chitral, northern Pakistan, lies within the Hindu Kush range, approximately 50 km to the northwest of the Main Karakoram Thrust (MKT), which marks the suture zone between the Kohistan complex and Asian plate (Fig. 1). The rocks around Miniki Gol, i.e., the study area mostly belong to the Arkari Formation of probable Jurassic age. These dominantly metasedimentary rocks include garnet-mica schist, graphitic schist, carbonaceous material, phyllite, psammite, calc-silicate quartzite and a thick unit of marble. The garnet-mica schist locally contains patches of tourmalinite.

The rocks of the Arkari formation have undergone at least two phases of deformation and metamorphism that are related to continent-arc collision during the Cretaceous and Eocene, respectively (Leake et al., 1989). A two-mica leucogranite has also intruded the rocks of the Arkari Formation. The pegmatitic phase of this granitic pluton contains xenloliths of metamorphosed pelitic rocks of the Arkari formation.

The calc-silicate and tourmalinite units of the Arkari Formation host the tungsten mineralization at Miniki Gol (Figs. 1 and 2). Previous workers believe the mineralization to be metamorphic in origin (see Leake et al., 1989). Although the leucogranite and tungsten mineralization do not appear to be spatially associated at least at the surface, a possible genetic relationship between the two cannot be ruled out. Based on mineralogical investigation of mainly the silicate phases, the current study attempts to explore this possibilty for the genesis of scheelite mineralization and its host rocks including both the calc-silicate quartzite and tourmalinite.

2. REGIONAL GEOLOGY AND TECTONICS

The India-Asia collision has produced three spectacular mountain ranges, i.e., Himalayas, Karakoram and Hindu Kush. Paleomagnetic and sea-floor spreading data in the Indian ocean suggest that the Indian plate started moving towards Asia at least 130 Ma ago (Powell, 1979). The collision between Kohistan arc and Karakoram terrane occurred between 100 and 80 Ma ago along the Main Karakoram Thrust

(Coward et al., 1986; Pudsey, 1986), which corresponds to the initiation of the northward subduction and consumption of the Tethys ocean. Subduction of the Indian plate continued in the direction of north and northeast and the final contact of the Indian plate with the Asian plate along the Main Mantle Thrust took place about 50 Ma ago (Molnar and Tapponnier, 1975; Petterson and Windley, 1985; Coward et al., 1986). To accommodate the post-collisional northward movement of India, three basic models have been proposed; crustal shortening and thickening (England and Mckenzie, 1982), underthrusting of India beneath Asia (Barazangi and Ni, 1982), and lateral eastward expulsion of Asia (Molnar and Tapponnier, 1975). The subduction and the subsequent crustal shortening and thickening have led to Barrovian type metamorphism followed by the intrusion of granodiorite and leucogranite within these two plates.

The Kohistan terrane, believed to be an intra-oceanic island arc resulting from the subduction related magmatic activity of the Tethys ocean, is bounded by major thrusts, i.e., the Main Mantle Thrust or Indus suture to the south and the Main Karakoram Thrust or Shyok suture to the north (Fig. 1). The Karakoram plate (Fig. 1) extends through northern Pakistan, northern Ladakh and western Tibet (Desio and Zanettin, 1970). Within the central Karakoram three main tectonic zones from north to south are recognised: a northern Karakoram terrane, the axial Karakoram batholith and the Karakoram metamorphic complex (Rex et al., 1988).

3. GEOLOGY OF THE MINIKI GOL AND SURROUNDING AREAS

The Hindu Kush terrane merges into western Karakoram along the Pak-Afghan border near Chitral (Fig. 1). The terrane, in the easternmost part of which lies the investigated area, stretches southwestward from the Pamirs in Russia across the north-western extremities of Pakistan and passes into Afghanistan. Based on the stratigraphical sequence and structural evolution, Pudsey et al. (1985) divided the geology of Western Karakoram and Hindu Kush in Chitral and surrounding areas into two tectonic units: (1) the Central unit between the Reshun Fault and MKT, and (2) the Northwestern unit between Pak-Afghan border and the Reshun Fault. The Central unit, predominantly composed of Paleozoic-Mesozoic metasediments, forms a 20–40 km strip and consists of Gahiret Limestone, Koghozi greenschist, Chitral Slate and Shoghor Limestone. The Northwestern tectonic unit, extending probably up to the Pamirs (Fig. 1; Pudsey et al., 1985), has been divided into Shogram Formation, Wakhan Formation, Sarikol Shale, and Lun Shales (Hayden, 1915; Desio, 1959; Calkins et al., 1981; Pudsey et al., 1985; Buchroithner and Gamerith, 1986). Later, Leake et al. (1989) subdivided the Northwestern unit into three fault-bounded lithostratigraphic formations namely the Sewakht Formation, Lutkho Formation and Arkari Formation (Fig. 1). The Arkari Formation, which extends up to the northwest of the Tirich Mir pluton, hosts the tungsten mineralization.

4. TUNGSTEN MINERALIZATION

Scheelite in the study area mainly occurs in the calc-silicate quartzite and subordinate tourmalinite. Although minor occurrences and showings of the mineralization extend up to the Garam Chashma area, the best grade tungsten mineralization occurs in a 2–3 km long belt/ zone in the vicinity of Miniki Gol (Figs. 1 and 2).

Scheelite occurs as discontinuous patches, stringers and

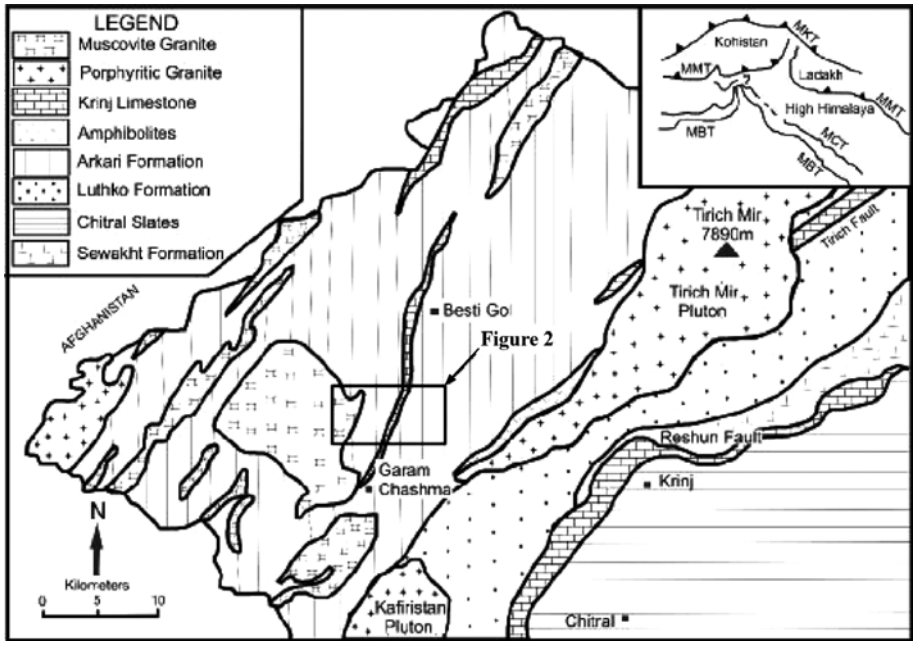

Fig. 1. Geological map of the Garam Chashma area showing Arkari Formation that hosts tungsten mineralization (after Leake et al., 1989).

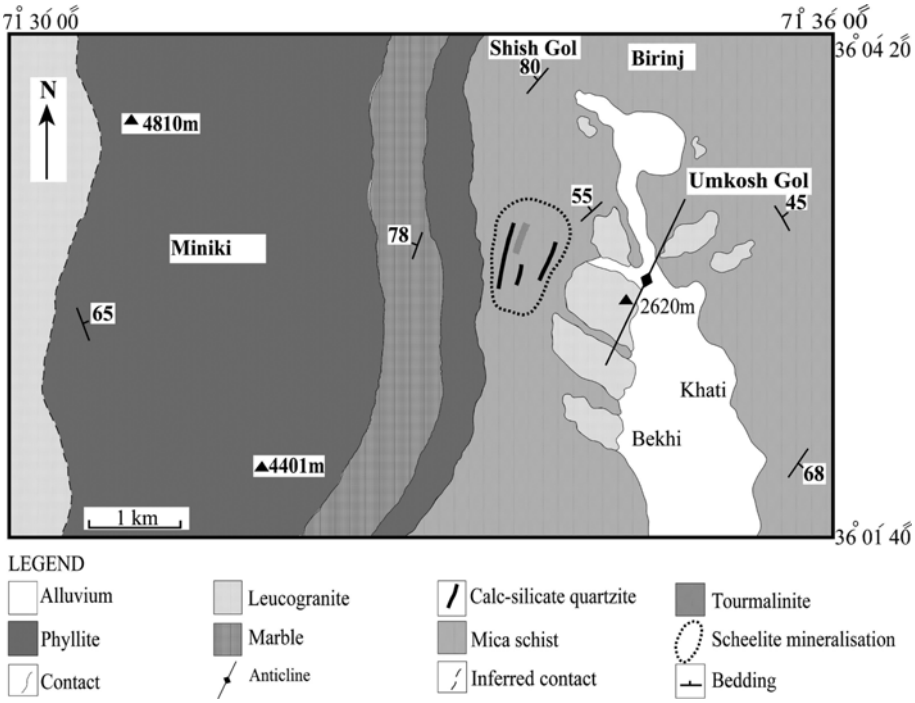

Fig. 2. A simplified geological map of the Miniki Gol and surrounding area.

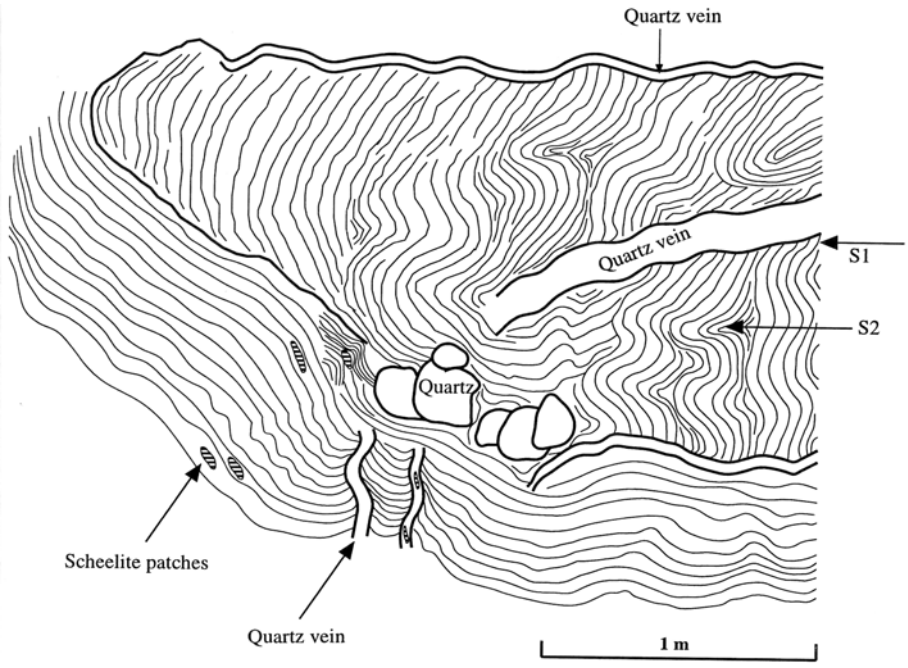

Fig. 3. Sketch of tourmalinite indicating overprint foliation (S1), crenulation cleavage (S2), quartz veins and scheelite patches. Note that some scheelite grains are emplaced within the quartz veins and S2 foliation.

conformable small veins within the calc-silicate quartzite and can be considered as stratabound type. In the tourmalinite, it occurs as finely disseminated grains as well as lenses (Fig. 3). The Miniki Gol scheelite mineralization seems to be structurally controlled. Its occurrence in the drag folded sections and along the axial planes of S2 suggests that it developed during the second phase of deformation when the Miniki Gol leucogranite also was intruded. The scheelite is intergrown with clinozoisite in the calc-silicate quartzite and with tourmaline of the tourmalinite. A minor amount of scheelite also occurs as veins apparently cutting across some of the early-formed main clinozoisite phase. Other ore minerals associated with scheelite include pyrite (partly altered to goethite), chalcopyrite, pyrrhotite and melnikovite (Leake et al., 1989).

5. SAMPLES, ANALYTICAL TECHNIQUES AND CONDITIONS

During extensive fieldwork in the study area, a total of about 294 rock samples representing almost all the lithological

types were collected. All these samples were studied petrographically through megascopic and microscopic examinations. Selected samples representing the calc-silicate rock, psammite, mica schist, tourmalinite and leucogranite were made into polished thin sections for detailed investigation with scanning electron microscope (SEM) and electron microprobe.

The analyses were performed in the University of Leicester (UK) through Jeol Superprobe model JXA-8600 with an on-line computer for ZAF corrections. Quantitative analyses were obtained using natural and synthetic standards and wavelength dispersive system under the following operating conditions: 15 kV (25 kV for the scheelite analyses) accelerating voltage; 30×10^{-9} A probe current; 20 (2×10) seconds peak, 10 (2×5) seconds negative background and 10 (2×5) seconds positive background counting times. The diameter of the X-ray beam varied according to the type, nature and grain size of the analysed phase. Except plagioclase (15 μm) and garnet (10 μm), 5 μm diameter was used for most of the silicate and oxide phases.

The silicate phases and some oxides were analysed for major and minor oxides including SiO_2, TiO_2, Al_2O_3, FeO, MnO, MgO, CaO, Na_2O, K_2O, Cr_2O_3 and NiO. Scheelite was analysed with a program consisting of CaO, WO_3, MoO_2, SnO_2, FeO, MnO, MgO, Y_2O_3, TiO_2, ZrO_2, Nb_2O_5, and Ta_2O_5. Based on measurement of Zr in pure tungsten metal, 0.4% ZrO_2 was deduced from the corresponding estimated value in each of the scheelite analyses.

The following standards were used during the microprobe analyses: wollastonite (natural for Si and Ca); rutile (natural for Ti); jadeite (natural for Al and Na); magnetite (synthetic for Fe); rhodonite (natural for Mn); MgO (synthetic for Mg); microcline (natural for K); YF_3 (synthetic for Y). Pure synthetic metals were used for each of W, Mo, Sn, Cr, Nb, Ta and Zr. The accuracy of the ZAF correction is generally better than 2%.

6. PETROGRAPHY

6.1. Calc-silicate Rock

The calc-silicate rock that hosts most of the scheelite mineralization at Miniki Gol, consists of clinozoisite, quartz, calcic-amphibole, plagioclase, chlorite, biotite, calcite, sphene and garnet. In some of the samples, the clinozoisite reaches up to 60 modal % and is intergrown with scheelite grains. Some of the calc-silicate rocks are banded, with darker layers being mainly composed of amphibole, chlorite and clinozoisite. The non-banded or granular variety largely consists of quartz and clinozoisite. Scheelite grains mostly occur in the non-banded variety.

6.2. Tourmalinite

The occurrence of tourmalinite, a subordinate host rock for scheelite, is relatively rare in the study area. Distributed as small patches, it has been identified only at three locations within the mica schist in the vicinity of the leucogranite. The studied tourmalinite predominantly consists of tourmaline. The abundance of tourmaline is variable, and makes up to 80% by volume of some of the samples. The scheelite-bearing tourmalinite consists of tourmaline, garnet, quartz and ilmenite, together with traces of magnetite, pyrite and pyrrhotite. Scheelite here is associated with tourmaline and garnet. Garnet in the tourmalinite is mostly subhedral in form and contains abundant inclusions. The tourmaline needles and blades occur within the foliation but without any alignment of their long axes. They contain abundant inclusions that, according to Leake et al. (1989) may define a planar fabric.

6.3. Leucogranite and Pegmatite

Exposed at the mouth of Miniki Gol approximately 400 meters to the south-east of the mineralized zone (Figs. 1 and 2), the two-mica leucogranite is generally unmineralized and essentially consists of coarse-grained aggregates of two feldspars, quartz, muscovite, biotite, garnet, tourmaline and apatite in decreasing volume percentage. The biotite is locally replaced by chlorite. The grains of garnet are cracked thereby indicating intragranular deformation. Large flakes of muscovite in these leucogranites define a penetrative foliation (see Leake et al., 1989). Some pegmatite patches and pockets also occur within the leucogranite. In terms of mineralogy, the leucogranite and pegmatite are more or less similar, however, alteration leading to the formation of kaolin seems to be restricted to the latter.

7. MINERAL CHEMISTRY

7.1. Tourmaline

Tourmaline analyses from schist, leucogranite and tourmalinite mostly fall in the field of metapelite (Fig. 4a). Some analyses from schist and tourmalinite, however, plot in the compositional field of tourmaline from granite. Tourmaline in the study area clearly shows an iron-enrichment trend from leucogranite to pegmatite on the TiO_2-FeO-MgO triangular diagram (Fig. 4b). This trend can also be observed in the tourmaline from xenolith within the pegmatite and tourmalinite (Fig. 4b).

The analysed tourmaline shows a broad range of chemical composition, particularly in terms of Fe, Mg contents and thus falls along the schorl-dravite join (Fig. 4b). The negative correlation between FeO and MgO corresponds to the schorl-dravite solid solution series (Fig. 4c). TiO_2 in these tourmalines ranges from 0.01 to 1.17 wt%, reflecting colour variation; a brown colouration correlates with high Ti content (cf. Deer et al., 1986). A high content of Na_2O

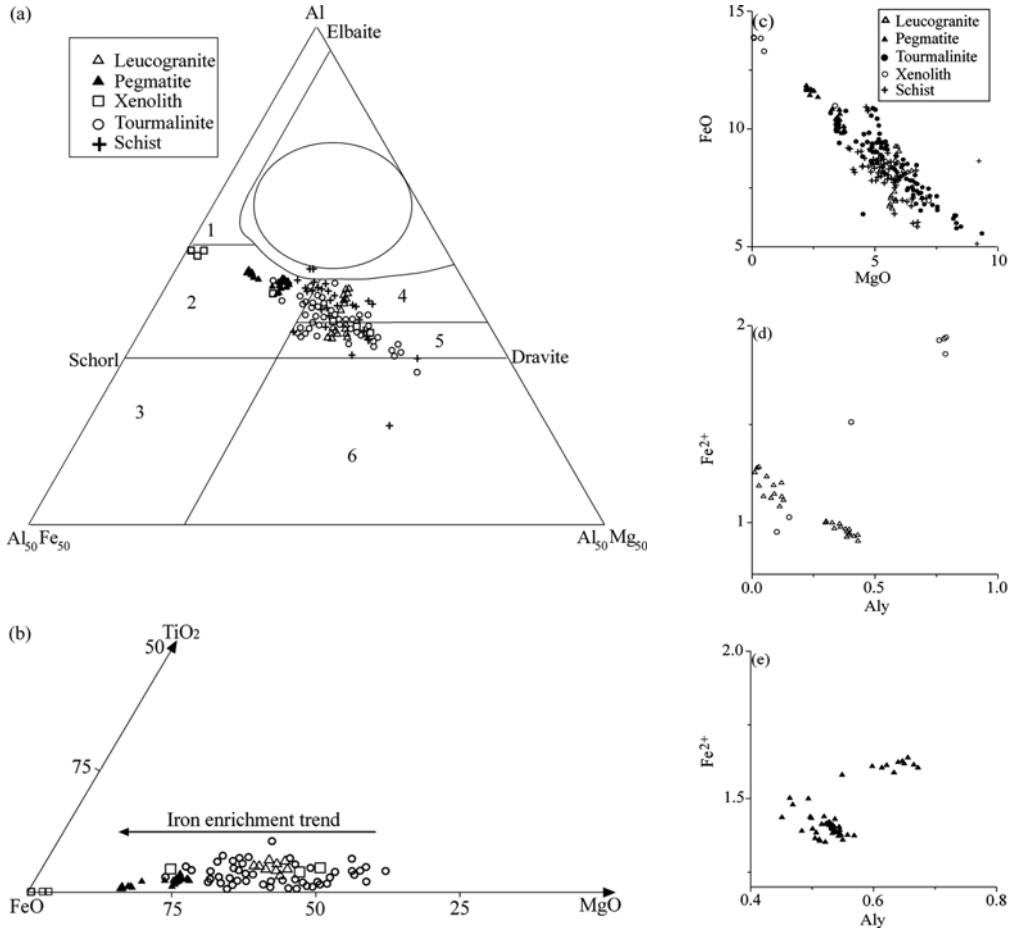

Fig. 4. Composition of tourmaline from the study area: (a) Al-Fe-Mg relations with fields of tourmaline (after Henry and Guidotti, 1985) from (1) Li-rich granitoid pegmatites and aplites, (2) Li-poor granitoids and their associated pegmatites and aplites, (3) Fe^{3+}-rich quartz-tourmaline rocks (hydrothermally altered granites), (4) metapelites coexisting with Al-saturating phase, (5) metapelites not coexisting with Al-saturating phase, (6) Fe^{3+}-rich quartz-tourmaline rocks, calc-silicate rocks, and metapelites; (b) TiO_2-FeO-MgO plot of tourmaline exhibiting iron enrichment trend; (c) FeO versus MgO plot; (d) and (e) relatioship of Fe^{2+} with Aly. Symbols shown in a and c also apply to the other plots.

is noted in the tourmaline of the tourmalinite and leucogranite, whereas tourmaline from the schist is relatively alkali-deficient (Table 1). Low levels of CaO are recorded both in leucogranite and pegmatite, whereas the Al_2O_3 content in the tourmaline of the pegmatite is generally higher than that of the leucogranite.

All the studied tourmalines contain excess alumina in the Y-site (Table 1). The relatively low alumina (Al_y) in the tourmaline from tourmalinite probably suggests that some Al may have been utilised in the formation of the intergrown spessartine-rich garnet. A negative correlation exists between Fe^{2+} and Al_y in the tourmaline of granite (Fig. 4d), whereas a positive correlation exists between these cations from xenoliths in the pegmatite (Fig. 4d) and the pegmatite itself (Fig. 4e). The concentration of FeO (average 8.54%) in the tourmaline of tourmalinite is higher than the tourmaline in schist (average 7.89%). Tourmaline in the schist, located farther away from granite intrusion, contains even lower FeO (averaging 7.14 wt%, Table 1).

It is interesting to note that tourmaline from the leucogranite plots within the compositional field for tourmaline from metapelite (Fig. 4a). This composition is markedly different from the Fe-rich schorl, which is considered to be the typical tourmaline of felsic plutonic rocks (Slack, 1982). This unusual compositional character of tourmaline from the Miniki Gol leucogranite is probably because it is xenocrystal in origin, i.e., derived as such from the wall rock. Alternatively, it indicates the original pelitic character of the melting source region for the parent magma to the host rock.

7.2. Garnet

About 400 spot analyses were performed on garnet in sixteen samples including garnet-mica schist, leucogranite,

Table 1. Representative average chemical composition of tourmaline

Lithology	Pegmatite		Leucogranite		Xenolith		Tourmalinite		Schist^C		Schist^R	
Analysis	M (51)[a]	Sd[b]	M (29)[a]	Sd[b]	M (7)[a]	Sd[b]	M (54)[a]	Sd[b]	M (3)[a]	Sd[b]	M (6)[a]	Sd[b]
SiO_2	36.12	0.19	36.2	0.16	36.21	0.43	36.93	0.43	36.35	0.33	36.71	1.31
TiO_2	0.34	0.1	0.75	0.14	0.31	0.37	0.47	0.23	0.49	0.04	1.03	0.17
Al_2O_3	34.01	0.25	32.32	1.12	33.51	1.25	31.6	0.74	32.48	0.73	30.39	1.01
Cr_2O_3	0.02	0.02	0.02	0.01	0.03	0.01	0.03	0.02	0.05	0.02	0.05	0.02
FeO*	10.54	0.64	7.75	0.83	11.49	3.07	7.55	0.93	7.14	0.83	7.19	0.53
MnO	0.11	0.03	0.06	0.02	0.31	0.21	0.07	0.03	0.02	0.01	0.04	0.02
MgO	3.25	0.5	5.89	0.24	2.61	3.18	6.73	0.93	5.72	0.16	6.7	0.25
CaO	0.15	0.04	0.61	0.18	0.18	0.24	0.5	0.37	0.36	0.15	1.07	0.33
Na_2O	2.02	0.12	2.12	0.06	1.82	0.31	2.27	0.26	1.98	0.09	1.75	0.21
K_2O	0.04	0.01	0.06	0.03	0.03	0.02	0.02	0.01	0.03	0.01	0.07	0.08
Total	86.6	0.27	85.78	0.31	86.5	0.29	86.17	0.55	84.62	0.37	84.99	0.57
Number of Cations on the basis of 24.5 (O)												
Si	5.947	0.016	5.961	0.035	5.998	0.013	6.047	0.036	6.025	0.056	6.088	0.176
Alt	0.053	0.016	0.041	0.031	0.006	0.01	0.001	0.005	0.011	0.018	0.016	0.023
Al_z	6.000	0.000	6.000	0.000	6.000	0.000	5.978	0.063	6.000	0.000	5.876	0.161
Al_y	0.546	0.053	0.233	0.156	0.539	0.314	0.118	0.094	0.336	0.115	0.052	0.081
Ti	0.043	0.013	0.093	0.017	0.038	0.045	0.058	0.029	0.060	0.004	0.128	0.021
Cr	0.002	0.002	0.002	0.002	0.004	0.001	0.004	0.003	0.007	0.003	0.006	0.003
Fe^{2+}	1.451	0.092	1.068	0.120	1.595	0.440	1.034	0.133	0.990	0.115	0.998	0.072
Mn	0.015	0.004	0.008	0.003	0.044	0.030	0.010	0.004	0.003	0.001	0.006	0.002
Mg	0.798	0.120	1.447	0.064	0.637	0.774	1.643	0.220	1.414	0.041	1.658	0.065
Ca	0.026	0.007	0.107	0.032	0.032	0.041	0.087	0.064	0.064	0.027	0.189	0.058
Na	0.645	0.037	0.678	0.023	0.584	0.092	0.722	0.081	0.635	0.031	0.563	0.071
K	0.009	0.002	0.012	0.006	0.007	0.004	0.004	0.002	0.006	0.002	0.014	0.016
Total	15.534	0.040	15.651	0.068	15.482	0.158	15.705	0.071	15.551	0.024	15.593	0.116

C = Core, R = Rim, M = Mean.
a = number of analyses; b = standard deviation.

tourmalinite and calc-silicate rock. Of these, 10 representative analyses are listed in Table 2. The analysed garnet from the mica schist is almandine-rich (52.4 to 84.7 mol % almandine) almandine-spessartine, whereas that from the leucogranite, pegmatite and tourmalinite is spessartine-rich spessartine-almandine (Table 2). Garnet from one of the calc-silicate rocks is, on the other hand, rich in the grossular component.

The MnO content of the almandine garnet from the studied schist ranges between 1.21 and 11.81 wt%, averaging ~6.31 wt%. Almandine garnet from the Miniki Gol granite and tourmalinite is relatively rich in MnO containing up to 16.62 wt% and 16.04 wt% MnO, respectively.

In contrast to that from leucogranite, garnet from both the mica schist and tourmalinite displays compositional zoning. Whereas CaO generally decreases from core to margin in the schist, it increases from core to margin in the garnet of tourmalinite (Table 2). The grossular content of garnet from leucogranite and, to a certain extent, schist is very low. In contrast, it is very high in the garnet from tourmalinite and scheelite-bearing calc-silicate rock (Table 2).

The Miniki Gol garnet data are plotted on the Mn-Mg-Fe triangular diagram of Miller and Stoddard (1981) (Fig. 5a). Except for a few analyses representing schist and tourmalinite, garnets from all the rocks in the studied area fall within the compositional field of igneous garnets. Moreover, garnet analyses from the two-mica granite and tourmalinite at Miniki Gol, plot above the line of 20 mol % spessartine (Fig. 5a), which Miller and Stoddard (1981) suppose to be the lower limit for two-mica granites. Except for the Ca content, which is higher in tourmalinite, garnets from the Miniki Gol leucogranite and tourmalinite are similar in composition (Table 2). In contrast, garnet from schist is characterized by higher pyrope contents.

MnO in the garnet of tourmalinite generally increases from core to margin (Fig. 5b, Table 2). In contrast, MnO decreases significantly from core to margin in most of the garnet grains from the schist (Fig. 5b, Table 2). Seemingly characteristic of the staurolite-grade pelitic schist (Woodsworth, 1977), this compositional zoning suggests preservation of

Table 2. Representative EPM analyses of garnet from the study area

Lithology	Schist		Schist		Tourmalinite		Leucogranite		Calc-sil. Rock	
Position	Core	Rim	Core	Rim	Core	Rim	Core	Rim	Core	Core
SiO_2	37.98	37.66	37.83	37.88	37.80	37.66	37.46	36.95	39.51	39.58
TiO_2	0.03	0.01	0.11	0.03	0.15	0.14	0.08	0.04	0.58	0.29
Al_2O_3	21.57	21.41	21.35	21.54	21.05	21.19	20.91	21.11	20.14	20.19
Cr_2O_3	0.03	0.03	0.04	0.00	0.01	0.04	0.03	0.01	0.13	0.14
FeO*	36.09	36.93	23.19	29.00	18.73	19.45	21.42	25.40	4.78	5.15
MnO	1.21	1.22	11.81	7.36	16.04	14.96	16.62	15.31	1.30	1.23
MgO	2.09	2.04	1.92	2.35	0.44	0.48	0.40	0.54	0.08	0.07
CaO	1.85	1.42	4.43	2.67	7.23	7.36	3.56	1.88	34.11	33.72
Na_2O	0.00	0.02	0.02	0.01	0.01	0.01	0.05	0.05	0.01	0.01
Total	100.85	100.74	100.7	100.84	101.46	101.29	100.53	101.29	100.64	100.38
Number of Cations on the basis of 12 (O)										
Si	6.06	6.04	6.03	6.03	6.02	6.00	6.05	5.98	6.02	6.05
Ti	0.00	0.00	0.01	0.00	0.02	0.02	0.01	0.01	0.07	0.03
Al	4.05	4.04	4.01	4.04	3.95	3.98	3.98	4.03	3.62	3.64
Cr	0.00	0.00	0.01	0.00	0.00	0.01	0.00	0.00	0.02	0.02
Fe^{2+}	4.81	4.95	3.09	3.86	2.49	2.59	2.90	3.44	0.61	0.66
Mn	0.16	0.17	1.59	0.99	2.16	2.02	2.28	2.10	0.17	0.16
Mg	0.50	0.49	0.46	0.56	0.11	0.11	0.10	0.13	0.02	0.02
Ca	0.32	0.24	0.76	0.46	1.23	1.26	0.62	0.33	5.57	5.52
Na	0.00	0.01	0.01	0.00	0.00	0.00	0.02	0.02	0.00	0.00
Total	15.91	15.93	15.95	15.95	15.99	15.98	15.95	16.01	16.09	16.09
Alm	83.1	84.7	52.4	65.8	41.6	43.3	49.2	57.4	9.6	10.4
Pyr	8.6	8.3	7.7	9.5	1.8	1.9	1.6	2.2	0.3	0.3
Gross	5.5	4.2	12.8	7.8	20.6	21	10.5	5.4	87.5	86.9
Spess	2.8	2.8	27	16.9	36.1	33.8	38.7	35	2.6	2.5

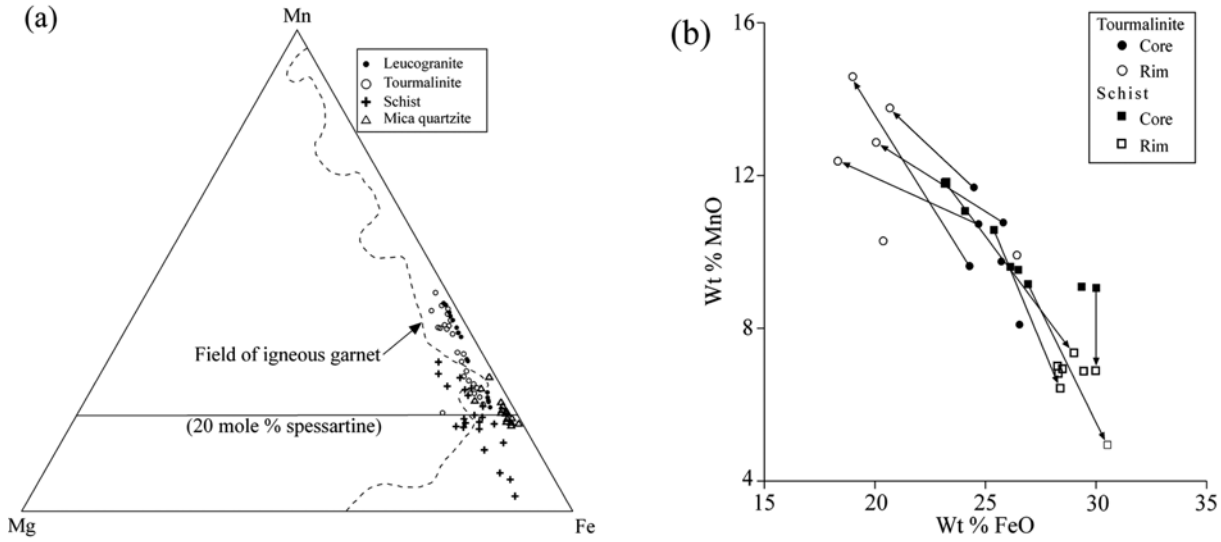

Fig. 5. Composition of garnet from the study area: (a) Mn-Mg-Fe plot superimposed with the compositional field of igneous garnet (Miller and Stoddard, 1981); (b) relationship between wt% MnO and FeO in garnet grains from tourmalinite and schist. Tie lines connect core and rim compositions within individual grains. Some of the tie lines are omitted for the sake of clarity. Note the totally opposite within-grain almandine-spessartine variation trends in the two rock types.

the original prograde regional metamorphic features of the studied schist within its garnet porphyroblasts presumably due to their large volume.

7.3. Clinozoisite-Epidote

Clinozoisite occurs in the calc-silicate quartzite and, although much rarely, in mica quartzite. This phase is totally absent from the mica schist of the Miniki Gol area, however, a few grains of epidote were identified in the chlorite-rich schist from Besti Gol, which is located ~8 km north of Miniki Gol.

In the granular calc-silicate rock, clinozoisite occurs as subhedral to euhedral grains associated with quartz and scheelite. The modal proportion of clinozoisite varies widely, and locally reaches up to 60%. The granular nature of clinozoisite with clear grain boundaries suggests that it is completely recrystallised. In one of the scheelite-bearing calc-silicate rock samples, the grains of clinozoisite show relics of lamellar twinning, thereby representing a stage of transition from its precursor, i.e., plagioclase.

Representative microprobe analyses of clinozoisite and epidote are presented in Table 3. Taking all the Fe as Fe_2O_3, the pistacite (Ps) content ($100Fe^{3+}/(Fe^{3+} + Al)$) of clinozoisite from the calc-silicate rocks generally ranges from 2.4 to 12.2 (Table 3), but occasionally approaches 16.6. This value is comparable to the epidote formed by the alteration of plagioclase (Tulloch, 1979). In contrast, the Ps content of epidote from chlorite-rich schist at Besti Gol ranges from 24.7 to 27.3 (Table 3), which seems to be the typical Ps of epidote from schists (Deer et al., 1986). Si and Al show an inverse relationship with Fe^{3+} but a weak positive correlation with Ca^{2+} (Fig. 6). About 40% of the clinozoisite grains show enrichment in Fe_2O_3 along their margins, thereby reflecting a later episode of retrograde metamorphism (Miyashiro, 1973). Such a type of compositional zoning is also noted in (1) epidote of the ancient geothermal systems (Shikazono 1984), (2) magmatic epidote and (3) epidote from many skarns (Deer et al., 1986; Farrow and Barr, 1992). The conversion of low-Fe^{3+}

Table 3. Representative EPM analyses of clinozoisite from calc-silicate rocks and epidote from greeschist

Lithology	CSR-B	CSR-Scheelite		CSR-Scheelite		G. Sch.
Position	Core	Core	Rim	Core	Rim	
SiO_2	39.53	39.63	39.14	39.79	39.18	37.77
TiO_2	0.14	0.02	0.30	0.20	0.17	0.56
Al_2O_3	28.99	32.37	29.58	29.34	28.67	22.59
Cr_2O_3	0.06	0.03	0.01	0.03	0.04	0.04
Fe_2O_3	5.66	1.12	3.79	5.22	5.46	11.95
MnO	0.17	0.03	0.13	0.26	0.24	0.23
MgO	0.03	0.01	0.06	0.05	0.08	0.01
CaO	24.34	24.91	24.20	24.24	24.05	23.77
Na_2O	0.01	0.02	0.02	0.01	0.32	0.00
K_2O	0.00	0.01	0.02	0.02	0.03	0.03
NiO	0.02	0.01	0.02	0.00	0.02	0.01
Total	98.95	98.16	97.27	99.16	98.26	96.96
Number of Cations on the basis of 25 (O)						
Si	6.11	6.03	6.10	6.12	6.11	6.21
Ti	0.02	0.00	0.04	0.02	0.02	0.07
Al	5.29	5.81	5.44	5.32	5.27	4.38
Cr	0.01	0.00	0.00	0.00	0.01	0.01
Fe^{3+}	0.73	0.14	0.49	0.67	0.71	1.64
Mn	0.02	0.00	0.02	0.03	0.03	0.03
Mg	0.01	0.00	0.01	0.01	0.02	0.00
Ca	4.03	4.06	4.04	4.00	4.02	4.19
Na	0.00	0.01	0.01	0.00	0.10	0.00
K	0.00	0.00	0.00	0.00	0.01	0.01
Ni	0.00	0.00	0.00	0.00	0.00	0.00
Total	16.22	16.07	16.15	16.19	16.29	16.53
Ps	12.2	2.4	8.3	11.2	11.9	27.3

Ps = Pistacite ratio $[100 \times Fe^{3+}/(Fe^{3+} + Al)]$.
CSR-B = barren calc-silicate rock; CSR-Scheelite = scheelite-bearing calc-silicate rock; G. Sch. = greenschist.

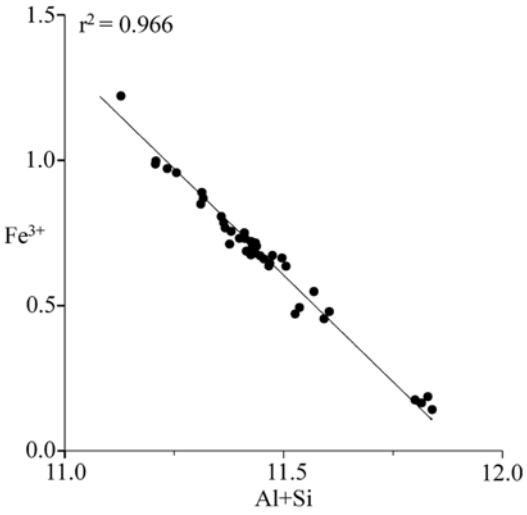

Fig. 6. Compositional variation in clinozoisit-epidote from the study area.

clinozoisite to high-Fe^{3+} clinozoisite (i.e., increase in Fe^{3+} content) reflects formation under decreasing temperature (see Deer et al., 1986; Chalokwu and Kuehner, 1992).

7.4. Sphene (Titanite)

Sphene mostly occurs in the calc-silicate rock and tourmalinite sequence in the study area, however, a few grains have also been found in mica schist. The chemical analyses of sphene from the calc-silicate rock are listed in Table 4. Because of its rather fine grain size, sphene from the schist could not be analysed and, therefore, compared with that from the calc-silicate rock.

The TiO_2 content of sphene in the calc-silicate rocks ranges from 27.63 to 36.43 wt% (mean 34.15 wt%). The inverse relationship between Ti and Al demonstrates their mutual substitution in the structure of sphene (Fig. 7a). The range of the TiO_2 content of the studied sphene is comparable with that from skarn and granitoid rocks (Lee et al., 1969; Deer et al., 1982).

Although characaterizd by variable and relatively higher Al contents (Table 4), most of the Miniki Gol sphene analyses from both the scheelite-bearing and barren calc-silicate rocks plot near the igneous and skarn field (Fig. 7b). However, some of the analyses plot away from the igneous and skarn field toward the Al-rich end, which is supposed to be the field for sphene of metamorphic origin (Tulloch, 1979).

In contrary to what was initially concluded, the occurrence of high-Al sphenes does not seem to be restricted to high-pressure rocks as higly aluminous sphenes, comparable to the ones presented here, occur also in low-pressure calc-silicate rocks from a number of localities, e.g., Egypt, Greece, Montagne Noire (France), the Salton Sea geothermal system, and Central Dronning Maud Land, Antarctica (Markl and Piazolo, 1999 and references therein). Hence chemical factors, especially the Al_2O_3/TiO_2 activity ratio in

Table 4. Representative EPM analyses of sphene from calc-silicate rocks

Analysis[a]	1	2	3	4	5
SiO_2	32.32	31.29	31.56	30.56	31.00
TiO_2	27.40	36.43	27.63	35.87	33.83
Al_2O_3	9.44	3.04	7.96	2.58	4.19
FeO*	0.54	0.24	1.28	0.24	0.58
MnO	0.05	0.04	0.07	0.07	0.01
MgO	0.04	0.01	0.74	0.01	0.02
CaO	30.12	29.04	26.78	29.50	28.03
Na_2O	0.00	0.03	0.03	0.01	0.04
K_2O	0.00	0.03	0.72	0.01	0.03
Total	99.91	100.15	96.77	98.85	97.73
Number of ions on the basis of four Si atoms					
Ti	2.550	3.500	2.630	3.530	3.280
Al	1.380	0.460	1.190	0.400	0.640
Fe^{2+}	0.060	0.030	0.140	0.030	0.060
Mn	0.010	0.000	0.010	0.010	0.000
Mg	0.010	0.000	0.140	0.000	0.000
Ca	3.990	3.980	3.640	4.140	3.880
Na	0.000	0.010	0.010	0.000	0.010
K	0.000	0.000	0.120	0.000	0.000
Total	11.990	11.980	11.870	12.110	11.880
O	19.240	19.710	19.040	19.850	19.480

[a]Whereas anaysis #1 is from a scheelite-free, all the others represent scheelite-bearing calc-silicate rocks.

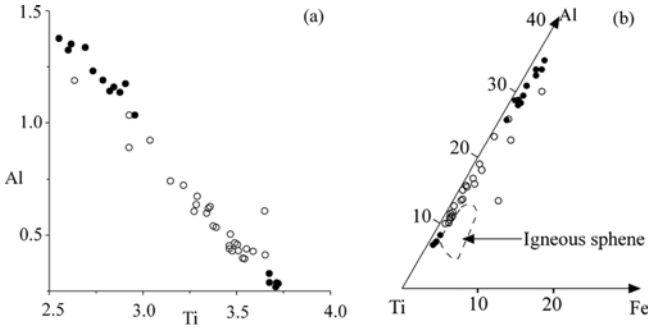

Fig. 7. Compositional characteristics of sphene from scheelite-bearing (filled circles) and scheelite-free (open circles) calc-silicate rocks from the study area: (a) relationship between Al and Ti contents; (b) Al-Ti-Fe ternary plot. Shown for the purpose of comparison is the compositional field of igneous sphene.

the host rocks and the F content of the coexisting fluid, rather than pressure appear to be controlling the Al content in sphene (Markl and Piazolo, 1999).

7.5. Scheelite

Scheelite from both the rock types, calc-silicate quartzite and tourmalinite, essentially cosists of CaO (20.5 wt%) and WO_3 (78.5 wt%) and is virtually free of Mo, Y, Ti, Sn, Fe and Mn. The outstanding feature of the scheelite from the investigated area is the presence of significant amounts of ZrO_2 (up to 0.46) and to a lesser extent Ta_2O_5 (up to 0.35 wt%). Similar values of Ta_2O_5 have also been reported from wolframite within a pegmatite from Thailand (Linnen and Williams-Jones, 1993).

As far as the authors are aware, significant amounts of ZrO_2 and Ta_2O_5 in scheelite have not been previously reported. Therefore, it may be of considerable interest to look at the petrogenetic implications of these components. Scheelite, particularly that from late-stage granites and pegmatites, is fairly rich in trace elements, e.g., Nb, Ta and V (Deer et al., 1992). Very high levels of zirconium and tantalum occur in scheelite from alkaline igneous rocks and from plutonic rocks relatively rich in soda (Deer et al., 1982; Tukiainen, 1988). Tantalum concentration in scheelite seems to increase with increasing degrees of differentiation of granitoid magmas (Boissavy-Vinau and Roger, 1980). Taylor (1965) argues that Ta is concentrated in Zr-containing minerals from post-magmatic environments, and that Zr^{4+} and Ta^{5+} replace W^{4+} and W^{6+}, respectively.

8. DISCUSSION

8.1. Source of Boron for the Formation of Tourmaline-rich Tourmalinite

Since the study area has suffered multiple episodes of deformation and metamorphism, it is very difficult to explain the genesis of the Miniki Gol tourmalinite in terms of its protolith and environment of formation. One of the major problems in this regard is the excessive supply of boron. The intrusion of leucogranite, which can be considered as a potential source of boron-rich fluids, in the vicinity of the tourmalinite further complicates the problem.

The presence of graphitic schist, carbonaceous material and a thick unit of calcite overlying the pelitic schist, apparently without structural discontinuity (Leake et al., 1989), supports a marine depositional environment for the Miniki Gol tourmalinite. The availability of Al in the exhalative environment for the formation of tourmaline on the sea floor in the vicinity of and within the submarine hydrothermal fluids has been discussed by Boström et al. (1969), Von Damm et al. (1985) and Slack et al. (1993). However, formation of the Miniki Gol tourmalinite through a submarine exhalative model is not plausible because of the following difficulties:

1. The limited strike length of the Miniki Gol tourmalinite (reported only at three locations within 2 km strike length) is inconsistent with the exhalative model. This is in sharp contrast to the Broken Hill exhalites, which extend for a distance of more than 330 km (Lottermoser, 1989).

2. Supportive evidences from typical sedimentary structures, which might indicate exhalation, do not exist. Although the possbility of obliteration of such features during metamorphism cannot be totally ruled out.

3. The close association and intergrowth between scheelite and tourmaline strongly suggest their simultaneous precipitation and, therefore, co-genetic relationship as well as a common source for both W and B. Whereas B occurs as B(OH)-4, BF-4 ions and undissociated B(OH)3 in natural waters, W is normally transported as tungstic acid, hydro- and simple tungstate ions (Willner, 1992). These lines of evidence manifest that the direct precipitation of both tourmaline and scheelite would not be possible during exhalation on the sea floor.

4. The absence of associated Sb and Hg (see Zahid, 1996) in the study area is inconsistent with exhalative activities (see also James and Ineson, 1993). The lack of cinnabar-stibnite mineralization with the Miniki Gol scheelite deposit also rules out the possibility of volcano-sedimentary origin for these rocks (Maucher, 1976).

Another possible explanation for the genesis of the Miniki Gol tourmalinite is through an evaporitic-sabkha model. However, this seems unlikely as the evidence for the former presence of evaporites or a lacustrine environment is lacking altogether. The absence of secondary halides also indicates a non-evaporitic environment.

A boron-rich clay does not seem to be a potential precursor either, as none of the known clay minerals contains more than 2000 ppm of boron (Slack et al., 1984). Such an abundance of boron would be sufficient for the formation of

only 9% tourmaline by volume (Plimer, 1986). In contrast, tourmaline in the Miniki Gol tourmalinites ranges up to 80 modal %.

To expalin the formation of the Miniki Gol tourmalinite through a metamorphic origin, whereby B is leached and brought to the site of deposition, has also got major problems. The leaching and transportation of boron over a large distance (few kilometres) and its subesquent concentration at a particular site of deposition probably would not be possible during progressive regional metamorphism.

It is important to mention here that tourmaline can be formed easily in situ by the diagenetic modification of evaporitic borate (Raith, 1988). However, as discussed by Leake et al. (1989), the Miniki Gol tourmalinite crystallised during the second phase of deformation. This clearly shows that sufficient B was not available in the first place for the formation of these tourmalinites during diagenesis.

From the discussion, presented above, it follows that only a magmatic activity can be considered as a potential source for the supply of sufficient quantities of B to account for the formation of the tourmalinite under investigation. The presence of leucogranite and pegamtite in close proximity to the tourmalinite lends further supports to such a thesis. Furthermore, the following mineralogical characteristics of tourmalinite and leucogranite are also conformable with this hypothesis:

1. The FeO# of tourmaline from tourmalinite is higher than that of the associated leucogranite, thereby reflecting an Fe-enrichment trend away from the granite as a result of late-stage evolved magmatic differentitaion (Bernard et al., 1985; Taylor et al., 1992). Such an iron-enrichment trend is also exhibited by the tourmalines from northern Portugal (Neiva, 1974), the Cornish granite and pegmatite (Lister, 1979), the Hub Kapong batholith of Thailand (Manning, 1982) and the Karagwe-Ankolean belt, Tanzania (Taylor et al., 1992). The average FeO# of the tourmaline (0.6) from the studied tourmalinite corresponds to that from magmatic hydrothermal (greisen-related) Sn-W deposits at Witkop and Van Rooi localities, South Africa (Pirajno and Smithies, 1992) and Kirwana Hill and Doctor Hill, New Zealand (Mackenzie, 1983). Furthermore,the reverse trend of chemical zoning, i.e., higher MnO in rims than cores, in the tourmaline grains from tourmalinite correspond to a metasomatic origin (Deer et al., 1982).

2. The uniformly high spessartine content of garnet from both the tourmalinite and leucogranite also suggests a genetic linkage between the two rocks. It is important to mention here that, besides being the product of a late-satge magmatic crystallization, garnet in leucogranite could also be xenocrystal in origin (Green, 1977; Miller and Stoddard, 1981; Stone, 1988). However, the markedly different composition, especially the low Mn content, of garnet from the country rocks (i.e., mica schists and their xenoliths in the pegmatites) as compared to that from the leucogranite, negates the xenocrystal origin for the garnet from leucogranite. The homogenous composition and relatively coarse grain size of garnets from the studied leucogranites further support their magamtic origin. Futhermore, spessartine-rich garnet with such a composition as the one occurring in the Miniki Gol leucogranite and tourmalinite is also believed to be post-magmatic in origin (Deer et al., 1982; Puziewicz, 1990).

3. Although being spessartine-rich, garnet from the studied tourmalinite also contains significant amounts of the grossular molecule (up to 30.5 mol %). Garnet with such a compositional character has also been reported from a scheelite-bearing skarn in Japan (Shimazaki, 1977).

8.2. Formation of the Calc-Silicate Rocks

The scheelite-hosting cal-silicate rock consists of clinozoisite, quartz, calcic-amphibole, plagioclase, chlorite, biotite, calcite, sphene and garnet. This modal composition is suggestive of a typical skarn assemblage, that is an originally calcareous rock transformed into a cal-silicate mineralogy by contact metasomatism. The following mineralogical characteristics of the rock under discussion further support this interpretation:

1. The very presence and composition of grossular garnet (containing up to 87.5 mol % grossular molecule) in the calc-silicate rock (Table 2) clearly indicates the Ca-rich character of the protolith. The drastically low grossular content of garnet from the other rock types, e.g., tourmalinite, negates the alternative explanation that Ca was supplied by the metasomatic solution.

2. The presence and very high modal abundance of clinozoiste (reaching up to 60%) in the calc-silicate rocks from the study area also indicate their skarn-like character. In contrast, the associated rocks, e.g., mica quartzite and garnet-mica schist, although contain abundant plagioclase, are totally devoid of clinozoisite.

3. The clinozoiste from the calc-silicate rock under discussion shows variation in the pistacite molecule thereby reflecting crystallization over a range of temperature. Clinozoisite with a very similar range of composition has been reported from calc-silicate veins (skarns) associated with the Land's End granite, Cornwall (Alderton and Jackson, 1978) and from pegmatite (Rao and Rao, 1971).

4. The composition of the Miniki Gol sphene, particularly that from scheelite-bearing calc-silicate rocks, fairly coordinates with igneous and skarn sphenes, indicating a hydrothermal activity related to igneous source (Fig. 7). According to Tulloch (1979), the metamorphic sphene is generally more aluminous (6–7 wt% Al_2O_3) than magmatic. However, some of the metamorphic sphene analyses from Victoria Range, New Zealand, compare well with igneous skarn. Aluminous sphene with up to 5.42% Al_2O_3 has also been recorded in a pegmatite from the Strzegom-Sobótka granitic massif, Poland (Janeczek and Sachanbinski, 1992).

8.3. Genesis of the Mineralization

As pointed out earlier, the occurrence of scheelite in the study area is largely restricted to the calc-silicate rock and tourmalinite. It has also been mentioned that scheelite is intergrown with clinozoisite in the former and tourmaline and garnet in the latter rock type. This leads one to conclude that scheelite has formed by the same process and precipitated from the same solutions that have been instrumental in the formation of the host rocks. As argued above, both the calc-silicate rock and tourmalinite formed as a result of a magmatic hydrothermal/contact metasomatic activity. The same process apparently also led to the formation of scheelite. Furthermore, the concentration of Zr and Ta (the elements usually related to igneous activity) in the studied scheelite indicates the involvement of a post-magmatic activity in the genesis of the calc-silicate rock. As mentioned in subsection 6.3 above, the Miniki Gol leucogranite itself is generally unmineralized, however, its average W content (5.3 ppm; Zahid, 1996) is higher than that of low-Ca granites (2.2 ppm W; Turekian and Wedepohl, 1961) and hence it might have acted as a source of W for sheelite mineraliztion. On the other hand, the average amount of W in the metasediments from the study area (2.6 ppm; Zahid, 1996) is almost similar to that of average shale (1.8 ppm; Turekian and Wedepohl, 1961) and thus does not support the possibility of a pre-granitic or exhalative source for tungsten concentration.

The cogenesis between W and Zr, shown by their association in the investigated scheelite, however does pose some problems. Zr is a compatible element and its mobility is limited particularly in igneous melts (Taylor, 1965). In contrast, W and Ta, being incompatible elements, are usually concentrated in the volatile-rich phase (Imeokparia, 1985). However, Rubin et al. (1993) have pointed out that Zr can be a highly mobile element in the fluorine-rich, peralkaline and peralumious hydrothermal systems. The high levels of fluorine in almost all the lithologies from the study area suggest the existence of a F-rich hydrothermal system.

The P-T conditions of crystallisation of the coexisting/associated phases in the host rock are also applicable to scheelite. Clinozoisite is believed to be stable under hydrothermal conditions at 2 Kb and up to 605 °C (Fyfe, 1960). Furthermore, the results of experimental work on the stability of clinozoisite suggest that it grows between 450 °C and 575 °C (Moody et al., 1985). Green (1977) has noted that garnet containing 20–25 mol % spessartine may crystallise in equilibrium with granitic liquid at depths as shallow as 12 km (~3 Kb pressure). Garnet from the studied leucogranite and tourmalinite contains up to 38.7 mol % (mean 29%) and 36 mol % spessartine (mean 26%), respectively. This suggests the crystallisation/equilibration of the Miniki Gol leucogranite and tourmalinite at 3 to 4 Kb pressure.

9. CONCLUSIONS

The discussion, presented above, leads to the followign broad conclusions:

1. The modal mineralogy and mineral-chemical composition of the calc-silicate rock, the dominant host to scheelite mineralization, suggest that it is a typical skarn assemblage.
2. The very tourmaline-rich tourmalinite that acts as a minor host to scheelite mineralistion, appears to have formed by boron metasomatism.
3. The dominant process responsible for the formation of both these scheelite-hosting rocks seems to be contact metasomatism associated with the intrusion and solidification of the Miniki Gol leucogranite.
4. As the scheelite is intergrown with some of the phases in both the calc-silicate rock and tourmalinite, the tungsten mineralization appears to be also a result of the same process of contact metasomatism that formed its host rocks.

ACKNOWLEDGMENTS: The Association of Commonwealth Universities in UK financed this study. Mr. Colin Cunnigham prepared the polished thin sections whereas Mr. Rob Wilson helped in performing the probe analyses at the Department of Geology, University of Leicester, UK.

REFERENCES

Alderton, D.H.M. and Jackson, N.J., 1978, Discordant calc-silicate bodies from the St. Just aureole, Cornwall. Mineralogical Magazine, 42, 427–434.

Barazangi, M. and Ni, J., 1982, Velocities and propagation characteristics of Pn and Sn beneath the Himalayan arc and Tibetan plateau: possible evidence for underthrusting of the Indian continental lithosphere beneath Tibet. Geology, 10, 179–185.

Boissavy-Vinau, M. and Roger, G., 1980, The TiO_2/Ta ratio as an indicator of the degree of differentiation of Tin granites. Mineralium Deposita, 15, 231–236.

Boström, K., Peterson, M.N.A., Joensuu, O., and Fisher, D.E., 1969, Aluminum-poor ferromanganoan sediments on active ocean ridges. Journal of Geophysical Research, 74, 3261–3270.

Buchroithner, M.F. and Gamerith, H., 1986, On the geology of the Tirich Mir area, central Hindu Kush (Pakistan). Jahrbuch der Geologischen Bundesanstalt, 128, 367–381.

Calkins, J.A., Jamiluddin, S., Bhuyan, K., and Hussain, A., 1981, Geology and mineral resources of the Chitral-Partsan area, Hindu Kush range, Northern Pakistan. United States Geological Survey Professional Paper, 716-G, 33.

Chalokwu, C.I. and Kuehner, S.M., 1992, Mineral chemistry and thermobarometry of a southern Appalachian amphibolite with epidote + quartz symplectite. American Mineralogist, 77, 617–630.

Coward, M.P., Windley, B.F., Broughton, R.D., Luff, I.W., Petterson, M.G., Pudsey, C.J., Rex, D.C., and Asif Khan, M., 1986, Collision tectonics in the NW Himalayas. In: Coward, M.P. and Ries, A.C. (eds.), Collision Tectonics. Geological Society London, Special Publication, 19, 203–219.

Deer, W.A., Howie, R.A., and Zussman, J., 1982, Rock-forming Minerals, 1A, Orthosilicates, 2nd Edition. Longman, London, 919 p.

Deer, W.A., Howie, R.A., and Zussman, J., 1986, Rock-forming

Minerals, 1B, Disilicates and ring silicates. Geological Society, London, 629 p.

Deer, W.A., Howie, R.A., and Zussman, J., 1992, An introduction to the rock-forming minerals, 2nd Edition. Longman, London, 696 p.

Desio, A., 1959, Cretaceous beds between Karakoram and Hindu Kush ranges (Central Asia). Rivista Italiana di Paleontologia e Stratigrafia, 65, 221–229.

Desio, A. and Zanettin, B., 1970, Geology of the Baltoro basin. Italian expeditions to the Karakoram (K2) and Hindu Kush (leader Desio, A.), Scientific Report, Section 11, 2. Brill, Leiden 308.

England, P.C. and Mckenzie, D.P., 1982, A thin viscous sheet model for continental deformation. Geophysical Journal of the Royal Astronomical Society, 70, 295–321.

Farrow, C.E.G. and Barr, S.M., 1992, Petrology of high-Al-hornblende- and magmatic-epidote-bearing plutons in the southeastern Cape Breton Highlands, Nova Scotia. Canadian Mineralogist, 30, 377–392.

Fyfe, W.S., 1960, Stability of epidote minerals. Nature, 187, 497.

Green, T.H., 1977, Garnet in silicic liquids and its possible use as a P-T indicator. Contribution to Mineralogy and Petrology, 65, 59–67.

Hayden, H.H., 1915, Notes on the geology of Chitral, Gilgit and the Pamirs. Records Indian Geological Survey, 45, 271–235.

Henry, D.J. and Guidotti, C.V., 1985, Tourmaline as a petrogenetic indicator mineral: an example from the staurolite grade metapelites of NW Maine. American Mineralogist, 70, 1–15.

James, D.W. and Ineson, P.R., 1993, Critique of exhalative hypothesis of tungsten skarn formation. Transactions of The Institution of Mining and Metallurgy (Section B: Applied Earth Sciences), 102, B205–B210.

Janeczek, J. and Sachanbinski, M., 1992, Babingtonite, Y-Al-rich titanite, and zoned epidote from the Strzegom pegmatites, Poland. European Journal of Mineralogy, 4, 307–319.

Leake, R.C., Fletcher, C.J.N., Haslam, H.W., Khan, B., and Shakirullah, 1989, Origin and tectonic setting of stratabound tungsten mineralization within the Hindu Kush of Pakistan. Journal of Geological Society London, 146, 1003–1016.

Lee, D.E., Mays, R.E., Van Loenen, R.E., and Rose, H.J.Jr., 1969, Accessory sphene from hybrid rocks of the Mount Wheeler mine area, Nevada. United States Geological Survey Professional Paper, 650-B, 41–46.

Linnen, R.L. and Williams-Jones, A.E., 1993, Mineralogical constraints on magmatic and hydrothermal Sn-W-Ta-Nb mineralization at the Nong Sua aplite-pegmatite, Thailand. European Journal of Mineralogy, 5, 721–736.

Lister, C.J., 1979, Quartz-cored tourmalines from Cape Cornwall and other localities. Ussher Society Proceedings, 4, 402–418.

Lottermoser, B.G., 1989, Rare-earth element study of exhalites within the Willyama Supergroup, Broken Hill Block, Australia. Mineralium Deposita, 24, 92–99.

Mackenzie, I.F., 1983, The geology and geochemistry of tungsten mineralisation at Doctor Hill and Falls Creek, Central Westland, New Zealand. M.Sc. thesis, Victoria University, Wellington, 162 p.

Manning, D.A.C., 1982, Chemical and morphological variation in tourmalines from the Hub Kapong batholith of peninsular Thailand. Mineralogical Magazine, 45, 139–147.

Markl, G. and Piazolo, S., 1999, Stability of high Al titanite from low-pressure calcsilicates in light of fuid and host-rock composition. American Mineralogist, 84, 37–47.

Maucher, A., 1976, The stratabound cinnabar-stibnite-scheelite deposits (discussed with examples from the Mediterranean region). In Handbook of Stratabound and Stratiform Ore Deposits (Wolf, K.H. Ed.). Elsevier, 10, p. 477–503.

Miller, C.F. and Stoddard, E.F., 1981, The role of manganese in the paragenesis of magmatic garnet: an example from the Old Woman-Piute Range, California. Journal of Geology, 89, 233–246.

Miyashiro, A., 1973, Metamorphism and Metamorphic Belts. Wiley, New York, 492 p.

Molnar, P. and Tapponnier, P., 1975, Cenozoic tectonics of Asia: effects of a continental collision. Science, 189, 419–426.

Moody, J.B., Jenkins, J.E., and Meyer, D., 1985, An experimental investigation of the albitization of plagioclase. Canadian Mineralogist, 23, 583–596.

Neiva, A.M.R., 1974, Geochemistry of tourmaline (schorlite) from granites, aplites and pegmatites from Northern Portugal. Geochimica et Cosmochimica Acta, 38, 1307–1317.

Petterson, M.G. and Windley, B.F., 1985, Rb-Sr dating of the Kohistan arc-batholith in the Trans-Himalaya of N. Pakistan, and tectonic implications. Earth and Planetary Science Letters, 74, 45–57.

Pirajno, F. and Smithies, R.H., 1992, The FeO/(FeO + MgO) ratio of tourmaline: a useful indicator of spatial variations in granite-related hydrothermal mineral deposits. Journal of Geochemical Exploration, 42, 371–381.

Plimer, I.R., 1986, Tourmalinites from the golden dyke dome, Northern Australia. Mineralium Deposita, 21, 263–270.

Powell, C.M., 1979, A speculative tectonic history of Pakistan and surroundings: some constraints from Indian ocean, In: Farah, A. and Dejong, K.A. (eds.), Geodynamics of Pakistan. Geological Survey of Pakistan, Quetta, p. 5–24.

Pudsey, C.J., 1986, The Northern Suture, Pakistan: margin of a Cretaceous island arc. Geological Magazine, 123, 405–423.

Pudsey, C.J., Coward, M.P., Luff, I.W., Shackleton, R.M., Windley, B.F., and Jan, M.Q., 1985, Collision zone between the Kohistan arc and the Asian plate in NW Pakistan. Transactions of the Royal Society of Edinburgh, 76, 463–479.

Puziewicz, J. 1990, Post-magmatic origin of almandine-spessartine garnet in the Strzeblow alaskite (Strzegom-Sobotka granitic massif, SW Poland). Neues Jahrbuch für Mineralogie, Monatshefte, 169, 157–192.

Raith, J.G., 1988, Tourmaline rocks associated with stratabound scheelite mineralization in the Austroalpine Crystalline Complex, Austria. Mineralogy and Petrology, 39, 265–288.

Rao, A.T. and Rao, K.S.R., 1971, Clinozoisite from pegmatite near Kandali, Nellore District, Andhra Pradesh. Indian Mineralogist, 12, 78–80.

Rex, A.J., Searle, M.P., Tirrul, A., Crawford, M.B., Prior, D.J., Rex, D.C., and Barnicoat, A., 1988, The geochemical and tectonic evolution of the central Karakoram, N. Pakistan. Philosophical Transations of the Royal Society London, Series A, 326, 229–255.

Rubin, J.N., Henry, C.D., and Price, J.G., 1993, The mobility of zirconium and other "immobile" elements during hydrothermal alteration. Chemical Geology, 110, 29–47.

Shikazono, N., 1984, Compositional variations in epidote from geothermal areas. Geochemistry Journal, 18, 181–187.

Shimazaki, H., 1977, Grossular-spessartine-almandine garnets from some Japanese scheelite skarns. Canadian Mineralogist, 15, 74–80.

Slack, J.F., 1982, Tourmaline in Appalachian-Caledonian massive sulphide deposits and its exploration significance. Transactions of The Institution of Mining and Metallurgy (Section B: Applied Earth Sciences), 91, B81–B89.

Slack, J.F., Herriman, N., Barnes, R.G., and Plimer, I.R., 1984, Stratiform tourmalinites in metamorphic terranes and their geologic significance. Geology, 12, 713–716.

Slack, J.F., Palmer, M.R., Stevens, B.P.J., and Barnes, R.G., 1993,

Origin and significance of tourmaline-rich rocks in the Broken Hill District, Australia. Economic Geology, 88, 505–541.

Stone, M., 1988, The significance of almandine garnets in the Lundy and Dartmoor granites. Mineralogical Magazine, 52, 651–658.

Taylor, S.R., 1965, The application of trace element data to problems in petrology. Physics and Chemistry of the Earth, 6, 135–213.

Taylor, R.P., Ikingura, J.R., Fallick, A.E., Yiming, H., and Watkinson, D.H., 1992, Stable isotope compositions of tourmalinites from granites and related hydrothermal rocks of the Karagwe-Ankolean belt, northwest Tanzania. Chemical Geology, 94, 215–227.

Tukiainen, T., 1988, Niobium-tantalum mineralisation in the Motzfeldt Centre of the Igaliko nepheline syenite complex, South Greenland. In: Boissonnas, J. and Omenetto, P. (eds.), Mineral Deposits within the European Community. Springer-Verlag, Berlin, 230–246.

Tulloch, A.J., 1979, Secondary Ca-Al silicates as low-grade alteration products of granitoid biotite. Contribution to Mineralogy and Petrology, 69, 105–117.

Turekian, K.K. and Wedepohl, K.H., 1961, Distribution of the Elements in some major units of the Earth's crust. Geological Society of America Bulletin, 72, 175–192.

Von Damm, K.L., Edmond, J.M., Measures, C.I., and Grant, B., 1985, Chemistry of submarine hydrothermal solutions at Guaymas Basin, Gulf of California. Geochimica et Cosmochimica Acta, 49, 2221–2237.

Willner, A.P., 1992, Tourmalinites from the stratiform peraluminous metamorphic suite of the Central Namaqua mobile belt, South Africa. Mineralium Deposita, 27, 304–313.

Woodsworth, G.J., 1977, Homogenization of zoned garnets from pelitic schists. Canadian Mineralogist, 15, 230–242.

Zahid, M., 1996, Genesis of stratabound scheelite and stratiform Pb-Zn mineralisation Chitral, Northern Pakistan, and its comparison with S-W England tin-tungsten deposits. Ph.D. thesis, University of Leicester, Leicester.

Manuscript received June 1, 2012
Manuscript accepted June 9, 2013